

Supplementary materials

pH-responsive antibacterial metal-phenolic network coating on hernia mesh

Rui Ding ^a, Pandi Peng ^a, Jingjing Huo ^a, Kun Wang ^a, Pengxiang Liu ^a, Hanxue Wu ^a,

Likun Yan ^{b, *}, Peng Li ^{a, *}

^aFrontiers Science Center for Flexible Electronics (FSCFE), Xi'an Institute of Flexible Electronics (IFE), Xi'an Institute of Biomedical Materials and Engineering (IBME), Northwestern Polytechnical University (NPU), Xi'an, 710072, China

^b Department of General Surgery, Shaanxi Provincial People's Hospital, Xi'an, 710068, China

***Corresponding Author**

Likun Yan – Department of General Surgery, Shaanxi Provincial People's Hospital, Xi'an, 710068, China; Email: likunyansurgery@163.com

Peng Li – Frontiers Science Center for Flexible Electronics (FSCFE), Xi'an Institute of Flexible Electronics (IFE) and Xi'an Institute of Biomedical Materials & Engineering (IBME), Northwestern Polytechnical University, Xi'an 710072, China; orcid.org/0000-0002-5876-2177; Email: iamppli@nwpu.edu.cn

Table S1 The surface elemental composition of all samples

Samples	Elements (atom %)		
	C	O	Cu
PP	99.70±1.61	0.30±2.40	/
PP-CT(1)	89.18±1.56	10.54±1.64	0.28±0.56
PP-CT(5)	87.91±1.61	9.89±1.71	2.20±0.58
PP-CT(10)	78.68±1.34	18.83±2.27	2.49±0.50

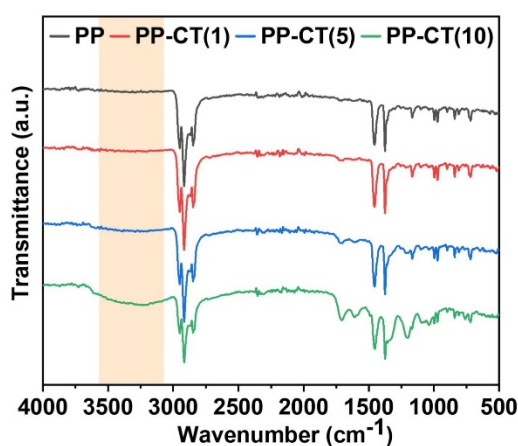


Figure S1. FTIR spectra of PP, PP-CT(1), PP-CT(5) and PP-CT(10).

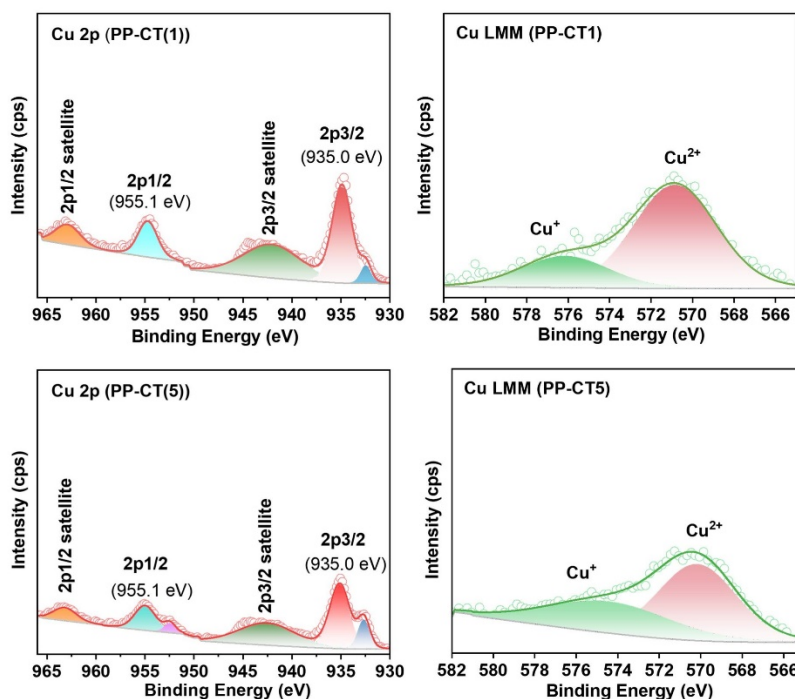


Figure S2. XPS high-resolution spectra of Cu 2p and Cu LMM of PP-CT(1) and PP-CT(5).

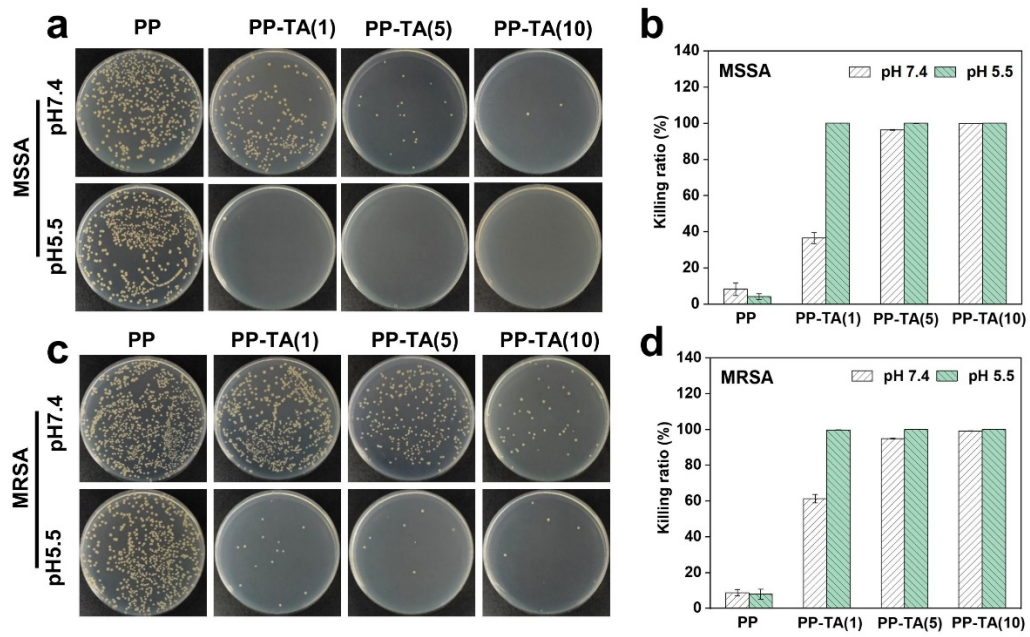


Figure S3. Colony formation of (a) MSSA and (c) MRSA, and the killing ratios against (b) MSSA and (d) MRSA after incubation 4 hours on the surfaces of pristine and TA coated PP meshes.

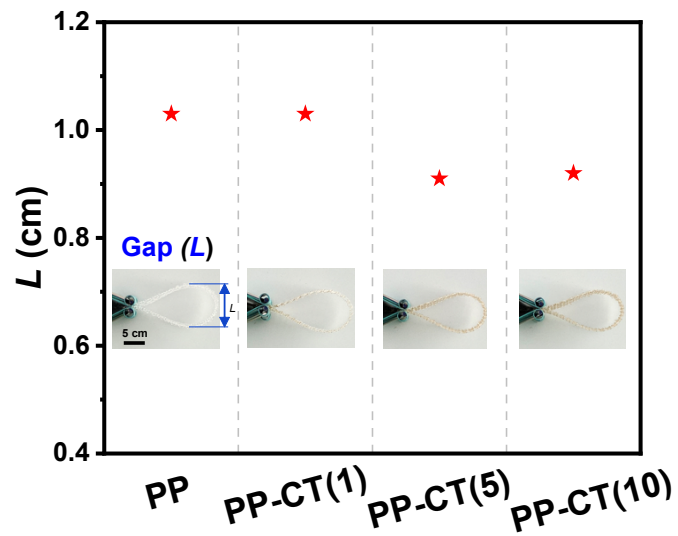


Figure S4. The gap length of folded pristine PP and CT coated PP meshes.

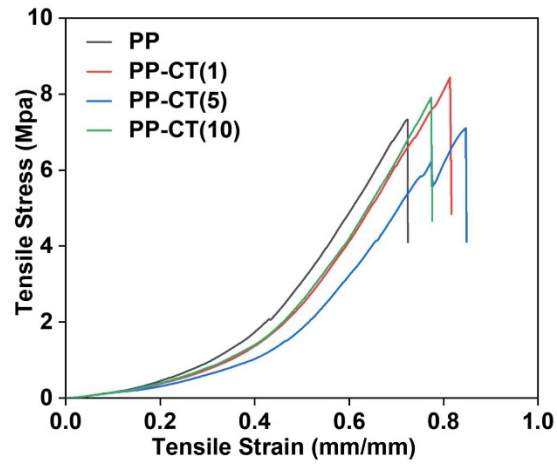


Figure S5. Tensile stress–strain curves of pristine and CT coated PP meshes